

Magnetic properties of mixed valence $\text{La}_{2/3}\text{Sr}_{1/3}\text{Mn}_{1-x}\text{T}_x\text{O}_3$ ($\text{T} = \text{Fe}, \text{Cr}$) manganites obtained by Pechini method

I BETANCOURT* and A MORALES-HERNÁNDEZ

Departamento de Materiales Metálicos y Cerámicos, Instituto de Investigaciones en Materiales, Universidad Nacional Autónoma de México, México D.F. 04510, México
e-mail: israelb@unam.mx

MS received 23 May 2012; revised 28 October 2012; accepted 26 November 2012

Abstract. Polycrystalline manganites of composition $\text{La}_{2/3}\text{Sr}_{1/3}\text{Mn}_{1-x}\text{T}_x\text{O}_3$ ($\text{T} = \text{Cr}^{3+}$ or Fe^{3+} , $x = 0.0$ – 0.10) were obtained by the Pechini method. Their magnetic properties exhibited a marked dependence on Fe/Cr content, with significant reduction of the magnetic moment per formula unit and their Curie temperatures. In addition, the magnetocaloric effect, determined by isothermal magnetization measurements, displayed a decreasing tendency with increasing Fe/Cr concentration. Results were interpreted on the basis of a deleterious effect on the double exchange interaction provoked by the presence of Fe^{3+} and Cr^{3+} ions within the crystal structure.

Keywords. Mixed valence manganites; magnetic manganites; magnetocaloric effect; Pechini method.

1. Introduction

Mixed valence manganites with perovskite structure and general formula $\text{A}_{1-x}\text{A}'_x\text{MnO}_3$ (where A is a trivalent cation such as La, Pr, Nd, Sm, Gd, Ho or Y, while A' stands for a divalent cation such as Ca, Sr, Ba and Pb), has been extensively studied because of their richness in transport and magnetic properties. Such phenomena includes a variety of couplings between charge, spin, orbital and vibrational degrees of freedom.^{1,2} In addition, these materials possess features of technological interest such as colossal magnetoresistance, magnetocaloric effect and unconventional insulator–metal transitions upon diverse external stimuli such as magnetic field, light, X-ray irradiation or current injection.^{3,4} Most studies focus on $\text{A} = \text{La}$ and on its partial substitution by divalent or monovalent cations.^{1,3,5–8} Other numerous reports describe the replacements of Mn by metallic species such as Fe, Co, Ni or Cr.^{3,9–11} For both cases, a strong correlation between electronic properties and the valence and the ionic radius of the doping atoms have been observed.^{1,2,4–6}

In particular, for $\text{La}_{1-x}\text{Sr}_x\text{MnO}_3$ systems, the presence of Mn^{3+} and Mn^{4+} cations (provoked by the inclusion of divalent cations such as Sr^{2+}) induces mobile holes in the e_g band near the Fermi energy, which

affects the electronic conduction and the superexchange interaction.^{1,2} The superexchange interaction causes antiferromagnetic coupling between magnetic moments in manganites and thus, moderate-to-low values for the magnetic moment per unit formula.^{1,2} This antiferromagnetic ordering can be progressively suppressed by the increment of the number of Mn^{3+} – Mn^{4+} pairs, which favours the double exchange interaction. The double exchange promotes ferromagnetic coupling between magnetic moments and hence, the enhancement of the magnetic moment per unit formula and the Curie temperature.^{12–15} The number of Mn^{3+} – Mn^{4+} pairs also influences the electronic structure of $\text{La}_{1-x}\text{Sr}_x\text{MnO}_3$ manganites, giving rise to a very rich phase diagram characterized by ample variations of critical temperatures associated to multi-phase transitions.^{1,16,17} Such transitions include paramagnetic insulator (PI), paramagnetic metallic (PM), spin-canted insulator (SCI), ferromagnetic insulator (FI), ferromagnetic metallic (FM) and antiferromagnetic metallic (AFM). Even first- to second-order magnetic phase transitions as a function of the Sr content have been reported.¹⁴ According to the phase diagram of $\text{La}_{1-x}\text{Sr}_x\text{MnO}_3$ manganites,^{1,16} the $x = 0.50$ point of Sr concentration lies at the border of the first order FM–AF transition, defining a so-called ‘bicritical point’.¹ This specific $\text{La}_{0.50}\text{Sr}_{0.50}$ proportion elicited a great interest from the scientific viewpoint because of the competing phases involved, namely FM, charge-orbital ordered AFM, and orbital-ordered AFM.¹

*For correspondence

Other interesting characteristic of manganites is the magnetocaloric effect (MCE), which refers to the isothermal magnetic entropy change (accompanied by an adiabatic temperature change) of a magnetic material under the application of an external magnetic field. This effect has been studied extensively in LaSr- and LaBa-based manganites because of the possibility for developing room temperature magnetic refrigeration technology based on their competitive cost of production, chemical stability and easy tailoring of magnetic properties.³ Although a significant number of compositional variations have been explored for La(Na,K,Ag)-, LaCa-, LaSr-, LaBa-, LaPb-, LaNd-, LaY- and LaLi-based manganites, reports concerning the effect of the systematic variation of Fe/Cr content on the MCE in $\text{La}_{2/3}\text{Sr}_{1/3}\text{MnO}_3$ manganites are much less numerous.^{3,18}

On the other hand, conventional synthesis of La-based manganites embraces in general some few variants of solid state reaction between oxides, nitrates or carbonates precursors at temperatures usually above 1200°C. An alternative and effective way to obtain manganites is a sol-gel variant known as ‘Pechini method’. This synthetic route was originally discovered for obtaining titanates, niobates and zirconates via polymeric precursors made from citric acid and ethylene glycol.¹⁹ In this method, an alpha hydroxycarboxylic acid (citric acid) is used to chelate with various cationic precursors by forming a polybasic acid. In the presence of a polyhydroxyl alcohol (ethylene glycol), the chelate reacts to form organic esters and water by-products. When the mixture is heated, polyesterification occurs and leads to a homogeneous sol in which metal ions are uniformly distributed throughout the organic matrix. Subsequent heating of the sol removes excess of solvents, leading to the formation of an intermediate resin. This solid resin is then heated to elevated temperatures to remove organic residuals, allowing the formation of the aimed stoichiometric compounds during pyrolysis. Due to uniform spreading of the ions, as well as the formation of small particles with narrow size distribution, the diffusion of cations affords the formation of oxides with high chemical homogeneity.^{19–22}

In this study, we present a systematic study on the magnetic properties, including MCE, of $\text{La}_{2/3}\text{Sr}_{1/3}\text{Mn}_{1-x}\text{T}_x\text{O}_3$ ($\text{T} = \text{Cr}^{3+}$ or Fe^{3+} and $x = 0.0, 0.025, 0.050, 0.075$ and 0.10) manganites, obtained by Pechini method. The selected La:Sr ratio lies within the FM zone (according to the phase diagram for $\text{La}_{1-x}\text{Sr}_x\text{MnO}_3$ manganites).^{1,16} For this $\text{La}_{2/3}\text{Sr}_{1/3}$ proportion with a single FM order, it is possible to establish correlations between magnetic properties and the valence state of the constituent transition-metal atoms,

since no additional effects between different competing magnetic phases are expected.

2. Experimental

The polycrystalline manganites series $\text{La}_{2/3}\text{Sr}_{1/3}\text{Mn}_{1-x}\text{Fe}_x\text{O}_3$ and $\text{La}_{2/3}\text{Sr}_{1/3}\text{Mn}_{1-x}\text{Cr}_x\text{O}_3$ ($x = 0.0, 0.025, 0.050, 0.075$ and 0.10) were prepared by the Pechini method with the following precursors: $\text{La}(\text{NO}_3)_3 \cdot 6\text{H}_2\text{O}$ (Fluka, $\geq 99.0\%$), $\text{Sr}(\text{NO}_3)_2$ (Fluka, $\geq 99.0\%$), $\text{Mn}(\text{NO}_3)_2 \cdot 4\text{H}_2\text{O}$ (Fluka, $\geq 97.0\%$), $\text{Cr}(\text{NO}_3)_3 \cdot 9\text{H}_2\text{O}$ (Fluka, $\geq 97.0\%$) and $\text{Fe}(\text{NO}_3)_3 \cdot 9\text{H}_2\text{O}$ (Mallinckrodt, $\geq 99.0\%$). The initial solution was prepared by mixing distilled water and the nitrates (properly weighed according to the specific composition), citric acid and ethylene glycol in the following molar proportion 1:5:4.3. The mixture was then dried at 50°C for 12 h. At this point, the resultant dried polymer was ground for a calcination treatment of 1100°C for 10 h in a muffle (Thermolyne 47900). Phase distribution analysis was done by X-ray diffraction (XRD) with Cu-K_α radiation, while microstructural characterization was carried out by scanning electron microscopy (SEM) in a Leica-Cambridge equipment operating at 20 kV. Concerning magnetic properties, the magnetic moment per formula unit for each compositional series was determined from hysteresis loops measured at room temperature in a vibrating sample magnetometer (VSM) at a maximum applied field of 15000 Oe, whereas the Curie temperature was established by means of magnetic thermogravimetric analysis (MTGA) in a thermobalance within the temperature range of 20–100°C at a heating rate of 10 K/min under an applied field of 0.20 T. In addition, the MCE was quantified by means of magnetic entropy variations $-\Delta S_M$, calculated from isothermal magnetization measurements with an applied magnetic field change of $\Delta H = 10000$ Oe, according to the following expression:^{3,17}

$$\Delta S_M = \int_{H_0}^{H_f} \left(\frac{\partial M}{\partial T} \right)_H dH \quad (1)$$

3. Results

3.1 Phase distribution and structural analysis

XRD diffractograms for selected compositions within the series $\text{La}_{2/3}\text{Sr}_{1/3}\text{Mn}_{1-x}\text{Fe}_x\text{O}_3$ and $\text{La}_{2/3}\text{Sr}_{1/3}\text{Mn}_{1-x}\text{Cr}_x\text{O}_3$ ($x = 0.0–0.10$) are shown in figure 1. For both cases, the main phase was identified

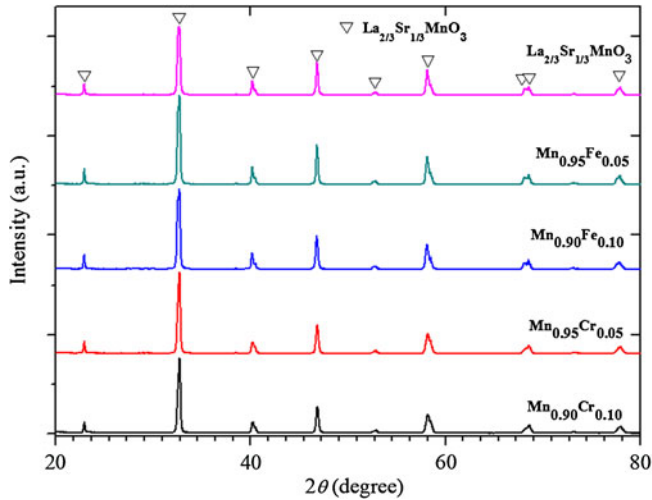


Figure 1. XRD diffractograms for selected compositions of the manganites series $\text{La}_{2/3}\text{Sr}_{1/3}\text{Mn}_{1-x}\text{T}_x\text{O}_3$ ($\text{T} = \text{Fe}$ or Cr).

as perovskite $\text{La}_{2/3}\text{Sr}_{1/3}\text{MnO}_3$ with rhombohedral symmetry and $R\bar{3}c$ space group, according to ICDD-PDF 01-089-4461. No secondary phases were observed in any case. Rietveld analysis²³ was performed to verify the formation of a single phase for each manganite series by using slow runnings from $2\theta = 25^\circ$ to 125° , as shown in figure 2 for the initial composition $\text{La}_{2/3}\text{Sr}_{1/3}\text{MnO}_3$ as example. Residuals for the weighted pattern $R_{\text{wp}}(\%)$ and the goodness of fit χ^2 across the compositional series resulted below 13% and 3.0%, respectively. These values are consistent with previous reports concerning similar materials.^{11,19,24} From the mathematical fitting, the unit cell parameters a and c (hexagonal coordinates) as a function of the Fe or Cr content were determined (figure 3). A minor variation

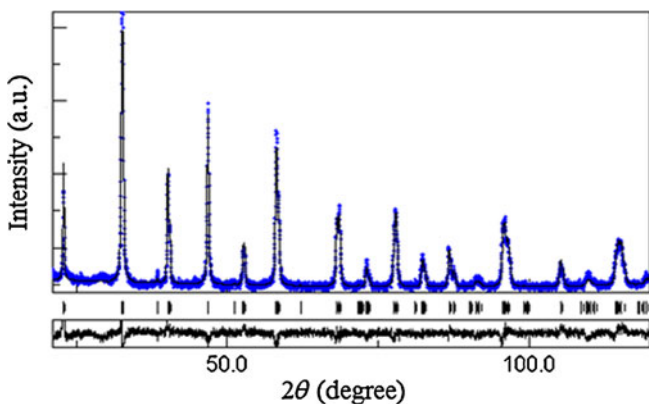


Figure 2. Experimental (dots) and calculated (solid) X-ray diffraction profiles for the $\text{La}_{2/3}\text{Sr}_{1/3}\text{MnO}_3$ sample. Tick marks below the diffraction pattern represent the allowed Bragg reflections. The difference profile is located at the bottom of the figure. The residuals for the fitting process were of $R_{\text{wp}}(\%) = 12.3\%$ and $\chi^2 = 1.9\%$.

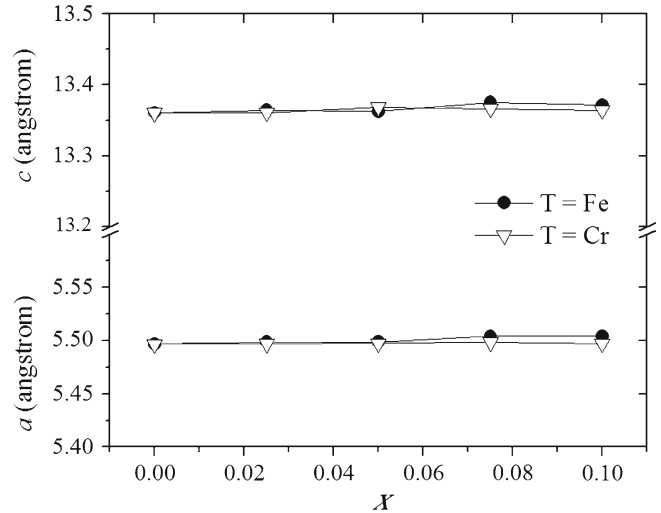


Figure 3. Unit cell parameters a and c (hexagonal coordinates) as a function of Fe/Cr content x for the compositional series $\text{La}_{2/3}\text{Sr}_{1/3}\text{Mn}_{1-x}\text{T}_x\text{O}_3$ (solid line does not represent a mathematical fit).

for both parameters is manifested for increasing Fe or Cr content. This marginal effect on the unit cell dimensions can be interpreted in terms of the very similar ionic radius of the cations Fe^{3+} and Cr^{3+} in octahedral coordination ($\langle r_{\text{Fe}^{3+}} \rangle = 0.64 \text{ \AA}$ and $\langle r_{\text{Cr}^{3+}} \rangle = 0.615 \text{ \AA}$)²⁵ compared with Mn^{3+} ($\langle r_{\text{Mn}^{3+}} \rangle = 0.65 \text{ \AA}$)²⁵ and Mn^{4+} ($\langle r_{\text{Mn}^{4+}} \rangle = 0.62 \text{ \AA}$).²⁵ Complementary SEM micrographs obtained with secondary electrons indicated the formation of a polycrystalline, randomly oriented distribution of polyhedral grains across the compositional series, as illustrated in figure 4 for the

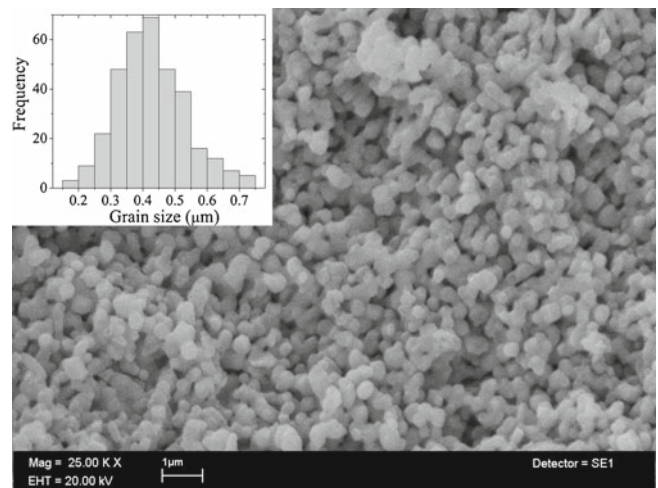


Figure 4. SEM image formed with secondary electrons, for the $\text{La}_{2/3}\text{Sr}_{1/3}\text{Mn}_{0.975}\text{Fe}_{0.025}\text{O}_3$ sample at a magnification of 20k. The associated grains size distribution histogram (shown as inset) was constructed by the intersection method employing several micrographs taken on different zones across the same sample.

$\text{La}_{2/3}\text{Sr}_{1/3}\text{Mn}_{0.975}\text{Fe}_{0.025}\text{O}_3$ manganite as an example. Much similar microstructural features were observed for the remaining compositions.

3.2 Magnetic properties

The hysteresis M – H loops for both compositional series, $\text{La}_{2/3}\text{Sr}_{1/3}\text{Mn}_{1-x}\text{Fe}_x\text{O}_3$ and $\text{La}_{2/3}\text{Sr}_{1/3}\text{Mn}_{1-x}\text{Cr}_x\text{O}_3$ are shown in figure 5(a) and (b), respectively. The values observed for the magnetic moment per formula unit are consistent with the magnetization of manganites with similar composition.²⁶ For both cases, a marked decreasing trend is observed, from 2.7 Bohr magneton (μ_B) per formula unit, f.u., to $0.9 \mu_B/\text{f.u.}$ for the Fe-containing manganites, and from 2.7 to $1.4 \mu_B/\text{f.u.}$ for the Cr-containing samples. These

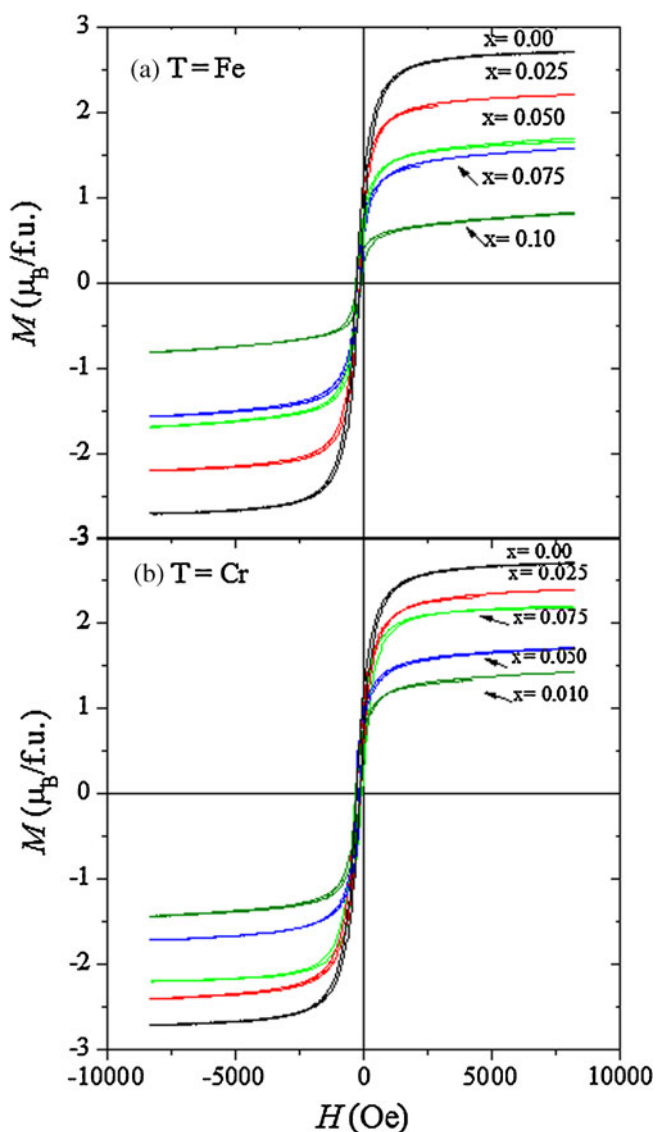


Figure 5. Hysteresis M – H loops for the compositional series $\text{La}_{2/3}\text{Sr}_{1/3}\text{Mn}_{1-x}\text{T}_x\text{O}_3$.

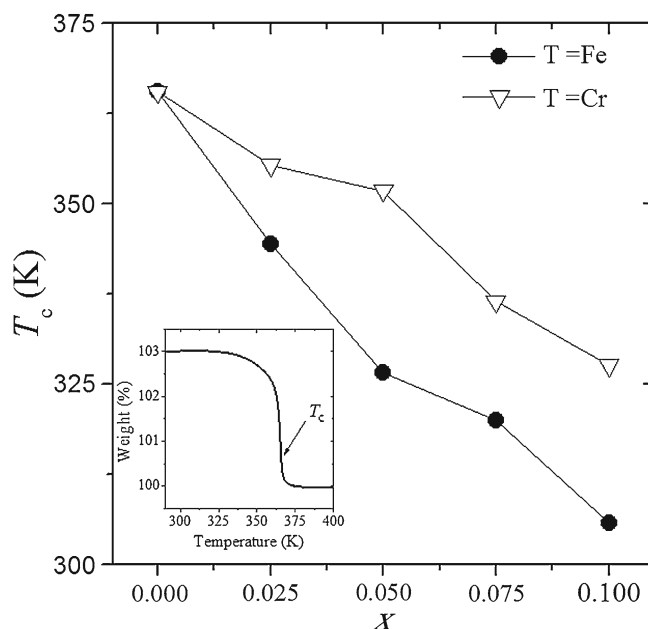


Figure 6. Curie temperature T_c as a function of Fe/Cr content x for the compositional series $\text{La}_{2/3}\text{Sr}_{1/3}\text{Mn}_{1-x}\text{T}_x\text{O}_3$ (solid line does not represent a mathematical fit). Inset: MTGA plot for the $\text{La}_{2/3}\text{Sr}_{1/3}\text{MnO}_3$ sample showing the Curie transition.

reductions in the magnetic moment per f.u. reflect the deleterious effect of the Fe/Cr substitution on the predominant double exchange interaction of the initial $\text{La}_{2/3}\text{Sr}_{1/3}\text{MnO}_3$ manganite in favour of the superexchange coupling, which promotes antiferromagnetic ordering. Complementarily, the Curie temperature T_c as a function of the Fe or Cr content is shown in figure 6. The Curie temperatures for both series of manganites display a diminishing tendency with increasing Fe or Cr content x . These T_c values were determined from

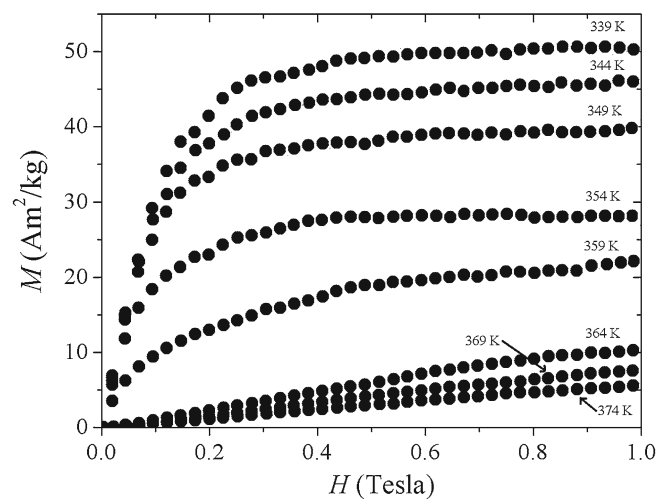


Figure 7. Isothermal magnetization curves for the $\text{La}_{2/3}\text{Sr}_{1/3}\text{MnO}_3$ manganite at a maximum applied field of 1.0 T.

MTGA, as shown for the $\text{La}_{2/3}\text{Sr}_{1/3}\text{MnO}_3$ manganite as inset in figure 6. The well-defined one-step shape of the MTGA curve indicates that all the grains undergo their Curie transition at the same temperature, which in turn reflects the excellent chemical homogeneity attained within the sample.

The reduction of these magnetic properties with Fe or Cr concentration is consistent with the incorporation of both atoms into the crystal structure of each manganites series (as suggested by XRD results), since the magnetic moment per f.u. and T_c are highly sensitive to the chemical composition. In addition, isothermal initial magnetization curves, determined for all the manganites across the compositional series (see figure 7 for the $\text{La}_{2/3}\text{Sr}_{1/3}\text{MnO}_3$ manganite as example), were measured from below and above the T_c indicated by MTGA results. From these curves, negative magnetic entropy ΔS_m calculated according to (eq. 1) are displayed in figure 8 for both compositional series. The

maximum in $-\Delta S_m$ is consistent with T_c determined by MTGA (figure 6) for all compositions, with a top value of -2.2 J/kgK for the original $\text{La}_{2/3}\text{Sr}_{1/3}\text{MnO}_3$ manganite, followed by a decreasing tendency for the maximum entropy variation as a function of the Fe or Cr concentration. Rapid reduction of the maximum in $-\Delta S_m$ is consistent with the significant diminution of the magnetic moment per f.u. for both compositional series, since high MCE values require a steep magnetization fall from large magnetizations at the Curie transition point.³ The observed $-\Delta S_m$ values compares very well with those reported for similar compounds.^{3,6,8}

4. Discussion

As mentioned in the ‘Introduction’, the increasing (or decreasing) number of $\text{Mn}^{4+}\text{-Mn}^{3+}$ pairs play a decisive influence on the electronic properties of $\text{A}_{1-x}\text{A}'_x\text{MnO}_3$ manganites through the creation (or suppression) of mobile holes affecting the superexchange interaction in favour (or against) of the double exchange interaction.^{1,2,26} For the present case, bearing in mind that no significant changes were detected for the unit cell parameters (figure 3), the marked reduction observed for the magnetic moment per f.u. and Curie temperature as a function of the Cr content x can be attributed to the weakening of the double exchange interaction as follows: The Cr^{3+} cations have the same electronic structure of Mn^{4+} , i.e., $[\text{Ar}]3d^3$ with three electrons at the lower t_{2g} level and 0 electrons at the higher e_g level. So, the progressive Cr concentration across the $\text{La}_{2/3}\text{Sr}_{1/3}\text{Mn}_{1-x}\text{Cr}_x\text{O}_3$ series implies an increasing number of cations with the $[\text{Ar}]3d^3$ configuration (i.e., Mn^{4+} configuration), which is equivalent to a progressive reduction of the number of Mn^{3+} cations, and hence, a reduced number of $\text{Mn}^{4+}\text{-Mn}^{3+}$ pairs. Reduction of these atom pairs favours the superexchange interactions between $\text{Cr}^{3+}\text{-O-Mn}^{4+}$, $\text{Cr}^{3+}\text{-O-Cr}^{3+}$ and $\text{Mn}^{4+}\text{-O-Mn}^{4+}$ cations, and thus, the deterioration of the magnetic properties of the $\text{La}_{2/3}\text{Sr}_{1/3}\text{Mn}_{1-x}\text{Cr}_x\text{O}_3$ series. The superexchange interactions being favoured between ions with empty e_g orbitals (i.e., $[\text{Ar}]3d^3$ configuration) in manganites were described in detail by Goodenough *et al.*²⁷ The decreasing tendency observed for $-\Delta S_m$ as a function of the Cr content x is a direct consequence of the diminution in the magnetic moment per f.u. since the MCE is very sensitive to magnetization variations.³

For the Fe-substituted manganites, deterioration of their magnetic properties can be explained in terms of the electronic structure of the Fe^{3+} and Mn^{3+} cations ($[\text{Ar}]3d^5$). This configuration comprises three electrons

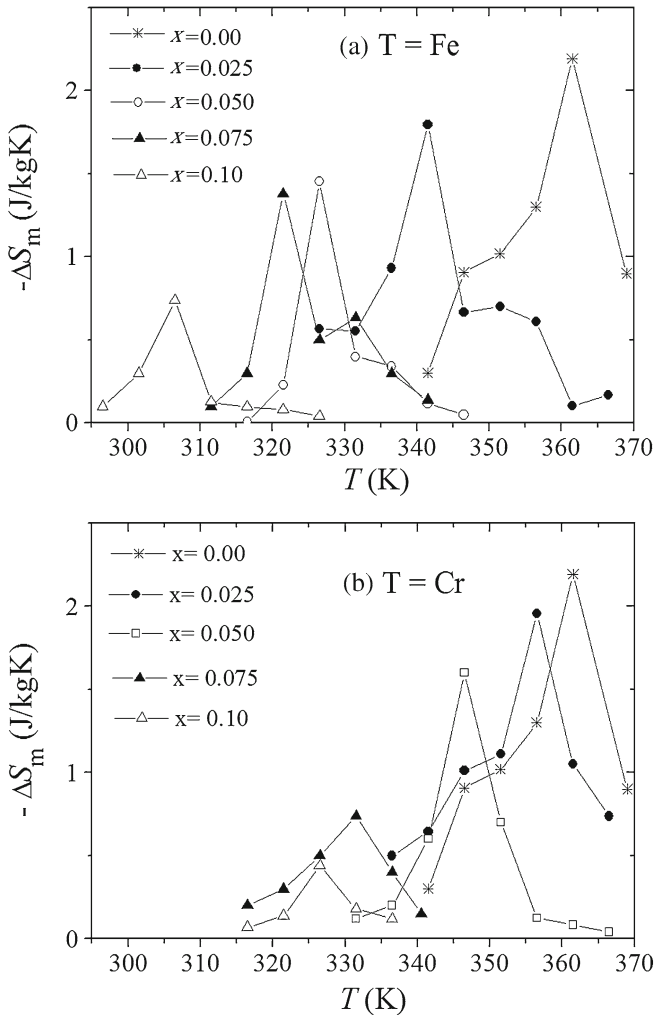


Figure 8. Magnetic entropy variation $-\Delta S_m$ for the compositional series $\text{La}_{2/3}\text{Sr}_{1/3}\text{Mn}_{1-x}\text{T}_x\text{O}_3$ (solid line does not represent a mathematical fit).

at the lower t_{2g} level and two electrons at the e_g level. However, according to Ahn *et al.*,²⁸ there is a poor overlap between the e_g bands of Fe^{3+} and Mn^{3+} ions (less than 3%),²⁸ which causes the hampering of the electron hopping from Mn^{3+} to Fe^{3+} . Since Fe^{3+} replaces Mn^{3+} within the perovskite structure, a reduction of the number of Mn^{3+} - Mn^{4+} pairs is expected, causing a depopulation of hopping electrons as well as the diminution of the number of available hopping sites. In consequence, the double exchange interaction (i.e., ferromagnetic ordering) is progressively suppressed in favour of the superexchange coupling (i.e., antiferromagnetic ordering) as the Fe content increases, leading to the worsening of the magnetic moment per f.u. and Curie temperature and hence, to the diminishing effect on $-\Delta S_m$. The valence state of the Fe^{3+} cation within the perovskite structure has been confirmed by means of Mössbauer spectroscopy in similar $\text{LaSr}(\text{MnFe})\text{O}_3$ manganites.¹⁸

5. Conclusion

The Pechini method was effective for preparing LaSr-based manganites with partial substitutions of Mn by Fe or Cr. The incorporation of Fe^{3+} or Cr^{3+} cations shows a shallow effect on the unit cell parameters, but a marked reduction of the magnetic properties and MCE due to significant weakening of the double exchange interaction (causing ferromagnetic ordering) in favour of the superexchange interaction (causing antiferromagnetic ordering).

Acknowledgements

IB thanks for financial support from research grant UNAM-PAPIIT IN104310. AMH is thankful for the scholarship support from UNAM-PAPIIT IN104310 and from research grant CONACYT-82358. Authors are also thankful to Adriana Tejeda, Omar Novelo and Esteban Fregoso (all from IIM-UNAM) for their valuable technical assistance.

References

1. Tokura Y 2006 *Rep. Prog. Phys.* **69** 797
2. Goodenough J B 2004 *Rep. Prog. Phys.* **67** 1915
3. Phan M-H and Yu S C 2007 *J. Magn. Magn. Mater.* **308** 325
4. Attfield J P 1998 *Chem. Mater.* **10** 3239
5. Hwang H Y, Cheong S-W, Radaelli P G, Marezio M and Batlogg B 1995 *Phys. Rev. Lett.* **75** 914
6. Yu J Y, Zhang S Y, Liu G H, Wu H Y and Wang L 2007 *Sol. Stat. Commun.* **142** 333
7. Sdiri N, Bejar M and Dhahri E 2007 *J. Magn. Magn. Mater.* **311** 512
8. Cheikh-Rouhou Koubaa W, Koubaa M and Cheikhrouhou A 2009 *Phys. Procedia* **2** 989
9. Ying Y, Eom T W, Dai N V and Lee Y P 2011 *J. Magn. Magn. Mater.* **323** 94
10. Dayal V and Keshri S 2007 *Sol. Stat. Commun.* **142** 63
11. Abdelkhalek S B, Kallel N, Guizouarn T, Peña O and Oumezzine M 2010 *J. Magn. Magn. Mater.* **322** 3416
12. Liu S P, Tang G D, Li Z Z, Ji D H, Li Y F, Chen W and Hou D L 2001 *Physica B* **406** 869
13. Bejar M, Dhahri R, El Halouani F and Dhahri E 2006 *J. Alloys Compd.* **414** 31
14. Mira J, Rivas J, Rivadulla F, Vazquez-Vazquez C and Lopez-Quintanella M A 1999 *Phys. Rev.* **B60** 2998
15. Liu S P, Tang G D, Li Z Z, Qi W H, Ji D H, Li Y F, Chen W and Hou D L 2001 *J. Alloys Compd.* **509** 2320
16. Urushibara A, Moritomo Y, Arima T, Asamitsu A, Kido G and Tokura Y 1995 *Phys. Rev.* **B51** 14103
17. Tishin A M and Spichkin Y E 2003 *The magnetocaloric effect and its applications* (Bristol-Philadelphia: Institute of Physics) Chapter 1
18. Zhang G and Lin J 2010 *J. Alloys Compd.* **507** 47
19. Pechini M P July 11 1967 U.S. Pat. No. 3330697
20. Kwon Y J 2002 *J. Ceram. Process Res.* **3** 146
21. Tai L W and Lessing P A 1992 *J. Mater. Res.* **7** 511
22. Baythoun M S G and Sale F R 1982 *J. Mater. Sci.* **17** 2757
23. Rietveld H M 1969 *J. Appl. Crystallogr.* **2** 65
24. Kumara Mangalam V R and Sundaresan A 2006 *J. Chem. Sci.* **118** 99
25. Shannon R D 1976 *Acta Crystallogr.* **A32** 751
26. Coey J M D, Viret M and von Molnar S 1999 *Adv. Phys.* **48** 167
27. Goodenough J B, Wold A, Arnott R J and Menyuk N 1961 *Phys. Rev.* **124** 373
28. Ahn K H, Wu X W, Liu K and Chien C L 1996 *Phys. Rev.* **B54** 15299